Ion-Molecule Reactions of Gas-Phase Chromium Oxyanions: $Cr_xO_yH_z^- + O_2$

A. K. Gianotto, B. D. M. Hodges, P. de B. Harrington,* A. D. Appelhans, J. E. Olson, and G. S. Groenewold

Idaho National Engineering and Environmental Laboratory, Idaho Falls, Idaho, USA

Chromium oxyanions, $Cr_xO_yH_z^-$, were generated in the gas-phase using a quadrupole ion trap secondary ion mass spectrometer (IT-SIMS), where they were reacted with O_2. Only CrO_2^- of the $Cr_1O_yH_z^-$ envelope was observed to react with oxygen, producing primarily CrO_3^-. The rate constant for the reaction of CrO_2^- with O_2 was ~38% of the Langevin collision constant at 310 K. CrO_3^-, CrO_4^-, and CrO_4H^- were unreactive with O_2 in the ion trap. In contrast, $Cr_2O_4^-$ was observed to react with O_2 producing $CrO_3^- + CrO_3$ via oxidative degradation at a rate that was ~15% efficient. The presence of background water facilitated the reaction of $Cr_2O_4^- + H_2O$ to form $Cr_2O_5H_2^-$; the hydrated product ion $Cr_2O_5H_2^-$ reacted with O_2 to form $Cr_2O_6^-$ (with concurrent elimination of H_2O) at a rate that was 6% efficient. $Cr_2O_5^-$ also reacted with O_2 to form $Cr_2O_7^-$ (4% efficient) and $Cr_2O_6^- + O$ (2% efficient); these reactions proceeded in parallel. By comparison, $Cr_2O_6^-$ was unreactive with O_2, and in fact, no further O_2 addition could be observed for any of the $Cr_2O_6H_z^-$ anions. Generalizing, $Cr_xO_yH_z^-$ species that have low coordinate, low oxidation state metal centers are susceptible to O_2 oxidation. However, when the metal coordination is >3, or when the formal oxidation state is ≥5, reactivity stops. (J Am Soc Mass Spectrom 2003, 14, 1067–1075) © 2003 American Society for Mass Spectrometry

Reactions of metal oxides with atmospheric gases are important because they modify the surface functionality, which in turn can alter the outcome of subsequent gaseous interactions. In the case of chromium, these changes can affect the macroscopic properties of toxicity and mobility in the atmosphere and in the geologic subsurface [1–3]. These behavioral attributes have motivated research into surface speciation of Cr-bearing surfaces, with the intent of correlating the explicit chemical form of the metal with transport and toxicity. Substantial research on Cr speciation has utilized desorption ionization mass spectrometry, either laser desorption mass spectrometry [4–16] or secondary ion mass spectrometry [14, 17–20]. These studies showed that indeed Cr surface speciation could be correlated with the mass spectral fingerprint generated by the desorption ionization studies. However, it was also noted that relatively subtle changes in the composition of the surface adsorbates (i.e., water) would significantly alter the population of the desorbed ions. These observations pointed out that desorbed ions underwent reactions with neutral gases in the vicinity of the desorption event, which influenced the appearance of the spectra [10, 12, 16], and complicated interpretation of surface speciation.

On the other hand, the reactions afford the opportunity to examine the reactivity behavior of ionic metal oxide species, provided that species-explicit, and time-dependent control can be exerted over the experiment. Since desorption ionization processes produce a variety of potentially reactive metal oxyanions, those gas-phase species that participate in aggregation or dissociation reactions can be studied. In particular, metal oxyanions containing low-coordinate metal centers are frequently produced in abundance: these are of particular interest because they are responsible for many significant reactions both in the gas phase and in the condensed phase [21–23].

Recently, Cr surface speciation has been revisited using an ion trap secondary ion mass spectrometer (IT-SIMS), which relies upon generation of gas-phase species by bombardment of surface species using a polyatomic primary particle [24–27]. The motivation behind reexamination of this topic was the possibility that the higher pressures extant in the ion trap (He bath gas) would serve to collisionally stabilize otherwise fragile molecular secondary ions [28], and would in the process amplify species-dependent mass spectral differences. However, the secondary $Cr_xO_yH_z^-$ ions were observed to react with ambient H_2O, and O_2 in the ion trap. A systematic study of the reactions with H_2O showed that ions containing undercoordinated metal

Published online August 4, 2003

Address reprint requests to Dr. G. S. Groenewold, Department of Chemistry, INEEL, P.O. Box 1625 MS 2208, Idaho Falls, ID, 83415-2208, USA. E-mail: gsg@inel.gov

*Center for Intelligent Chemical Instrumentation, Department of Chemistry and Biochemistry, Ohio University, Athens, OH 45701-2979

1044-0305/03/$30.00
doi:10.1016/S1044-0305(03)00410-0

Received February 18, 2003
Revised May 23, 2003
Accepted May 23, 2003

centers would undergo either addition or radical abstraction reactions [29]. These reactions would proceed in series until a Cr coordination number of 4 was reached, except for CrO_3^-, which was unreactive.

The reactions of the chromium oxyanions with O_2 were also significant, and the present study describes these in detail. The O_2 oxidation of small Cr-bearing species was previously examined using laser ablation in an O_2 atmosphere, with product isolation and analysis in a frozen argon matrix [30]. A suite of neutral products having the compositions $Cr_1O_{2\text{-}4}$ and $Cr_2O_{2\text{-}4}$ were identified using FTIR, and ab initio calculations suggested structures containing rhombic Cr_2O_2 structural units [30, 31]. O_2 reactions with ionic Cr oxide species were conducted by Bricker and Russell [32], who concluded that O_2 would bind with Cr carbonyl anions in a molecular fashion, but gas-phase studies of Cr oxyanions more typical of the condensed phase have not been conducted. Here, O_2 oxidation of $Cr_{1,2}O_yH_z^-$ species is examined using an ion trap SIMS instrument; this approach has been effective for elucidating reaction pathways and kinetics for ionic Al [33, 34], Si [34], and U oxides [35]. The results show that under the ambient conditions of the ion trap (1×10^{-4} torr He, 310 K), $Cr_{1,2}O_yH_z^-$ species containing low-coordinate, low oxidation state metal centers underwent oxidation.

Experimental

Instrumentation

Molecular secondary ions were sputtered into the gas phase within the IT-SIMS from powdered potassium dichromate (Baker Chemical, Phillipsburg, NJ) samples that were attached to the end of a 2.7 mm probe tip with double-sided tape (3M, St. Paul, MN). The IT-SIMS instrument used in this study is a modified Finnigan ITMS (Finnigan Corp., San Jose, CA) previously described [36]. Modifications include incorporation of a perrhenate (ReO_4^-) primary ion beam, an insertion lock for introduction of solid samples, and an offset dynode with multichannel plate detector. The primary ion gun and sample probe tip are collinear and located outside opposite end caps of the ion trap. The primary ion gun was operated at 4.5 keV and produced a ReO_4^- beam with a 1.25 mm diameter at a primary ion current ranging from 300 to 450 pA. The ReO_4^- beam was used because this type of ion beam is more efficient for sputtering larger cluster ions into the gas-phase compared to atomic particle bombardment [20, 24, 27, 37]. The data acquisition and control system uses the Teledyne Apogee ITMS Beta Build 18 software that controls routine ITMS functions and the filtered noise field (FNF) (Teledyne Electronic Technologies, Mountain View, CA). Data analysis was performed using SATURN 2000 software (version 1.4, Varian, Walnut Creek, CA).

A variable leak valve controlled the admittance of gaseous O_2 into the IT-SIMS for ion-molecule reaction experiments. Ion-molecule experiments were conducted at O_2 pressures of $\sim 1\text{–}2 \times 10^{-6}$ torr. Because the ion gauge response for O_2 is 0.87 of N_2 [38], ion gauge pressures were accordingly corrected when calculating rate constants. The He bath gas was operated at a corrected pressure of 1×10^{-4} torr. The IT-SIMS base pressure was $\sim 5 \times 10^{-8}$ torr.

IT-SIMS Parameters

A representative sequence of events for ion-molecule reactions has been previously reported [33]. For typical chromium oxyanion experiments, the ion trap was operated with a low mass cutoff of 40 u. Ionization times were adjusted to produce an acceptable number of ions (signal-to-noise $\geq \sim 100$) for O_2 reactivity experiments. During ionization the ReO_4^- beam was directed through the ion trap and onto the chromium oxide target. Ion isolation was performed at the same time as ionization (sample bombardment) by applying a notched FNF, where the frequencies of the notch corresponded to the natural frequency of the ion being isolated. This method resulted in ejection of ions whose natural frequencies do not fall within the notch. Because ion mass is correlated with frequency, mass selective ion isolation was accomplished.

The width of the ion isolation notch was nominally 1 u, although it was noted that the notch did not always completely exclude ions at adjacent masses. We strove to ensure that the abundances of ions at adjacent masses were $< 10\%$ of the abundance of the ion being selected for reaction. The presence of non-ejected ions at adjacent masses led to minor ambiguities arising from the inclusion of ^{53}Cr-bearing isotopic peaks in the isolation window, but did not influence the interpretation of any of the reaction results.

Once the ions were formed and isolated, ion-molecule reactions with O_2 began to occur. Because water vapor was present in the ion trap, it also participated in ion-molecule reactions [29]. Altering the duration of a delay period between the ionization/isolation event and the ion scan-out/detection enabled assessment of the extent of reaction.

After reaction, ions were scanned out of the ion trap using a mass selective instability scan with axial modulation [39]. Background spectra were collected for each sample. Seven spectra (each composed of the average of 20 scans) were averaged and background corrected to obtain final peak intensities. The relative standard deviation between averaged spectra was $\pm 5\%$.

Calculation of Rate Constants

The reactions examined were accurately described using pseudo-first order kinetics, as if they were bimolecular. A pseudo-first order approximation was appropriate because the concentration of O_2 was significantly greater than the concentration of the ions, and hence the O_2 concentration remained constant throughout the

reaction. Uncertainty in the accuracy of the O_2 concentration, especially at low pressure, was felt to be the principle contributor to the uncertainty of the rate constant calculations.

Because of collisions with the He bath gas, which is present in the ion trap to damp ion trajectories, the reactions are in fact termolecular: He and the other gases in the IT-SIMS serve to collisionally stabilize initially formed adducts [40]. The narrow range of operating pressures for trapping the anions in the IT-SIMS (1–2 $\times$ 10^{-5} torr) did not facilitate an extensive evaluation of the role of the He bath gas in these reactions. However, over the range of accessible He pressures, significant variations in the measured reaction rates were not observed. This suggested that the initially formed adducts were not particularly sensitive to small changes in the He pressure. The reactions behaved as apparent bimolecular processes [41, 42], and hence the rate constants are reported as such.

CrO_2^-, $Cr_2O_4^-$, and $Cr_2O_5^-$ all underwent a combination of consecutive and parallel reactions which made assignment of reaction pathways and calculation of individual rate constants difficult. A multivariate curve resolution approach [43] (MCR) was employed to identify reaction pathways in an unbiased fashion. Reactant and product ion relationships, and their general kinetic behavior, were determined using the MCR method SIMPLISMA [44]. Next, a hard-modeling approach that used an alternating least squares (ALS) regression [45, 46] was employed to generate concentration profiles starting from the MCR-derived kinetic model. Finally, a set of kinetic rate equations were fit to the concentration profiles obtained from ALS using the MATLAB 6.1 (Mathworks, Inc, Natick, MA) function FMINSEARCH, which uses a non-linear simplex optimization [47]. This method, referred to as the ALS method in the manuscript, was used because it eliminated bias in the assignment of reaction pathways, and provided reaction rates that were optimized to the actual data sets. A comprehensive description of the method is in preparation [43].

Reaction efficiency was evaluated by comparing measured rate constants with theoretical rate constants calculated using the Langevin rate constant theory [48, 49]. The Langevin collision constants were calculated using a reaction temperature (310 K) which was the average ion temperature for an ion in a typical trap as calculated by both Goeringer and McLuckey [50] and Gronert [51]. In the case of the water reactions the reparameterized average dipole orientation collision constant was used for calculating reaction efficiencies [49].

Results and Discussion

The negative secondary ion mass spectra of chromium (VI) oxide species acquired using the IT-SIMS (Figure 1) qualitatively resembled laser desorption and SIMS mass spectra reported previously in the literature, in that abundant envelopes of ions corresponding to $Cr_1O_yH_z^-$, $Cr_2O_yH_z^-$ and $Cr_3O_yH_z^-$ ion envelopes were recorded. In

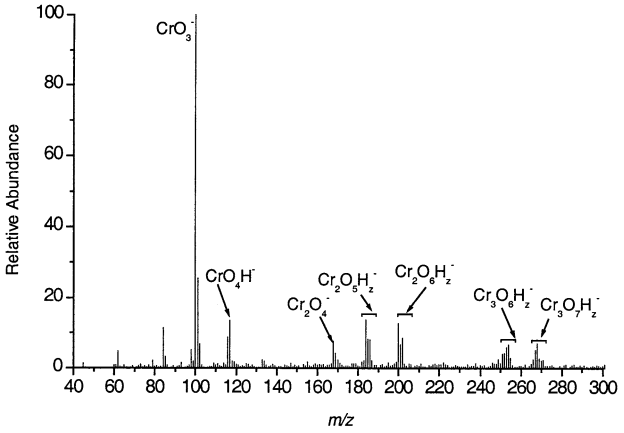

Figure 1. Anion IT-SIMS spectra of potassium dichromate sample acquired at 0.01s ionization time at 1.4 $\times$ 10^{-6} torr (ion gauge).

the $Cr_1O_yH_z^-$ envelope, the significant anions were observed at *m/z* 84 (CrO_2^-), *m/z* 100 (CrO_3^-), *m/z* 116 (CrO_4^-) and *m/z* 117 (CrO_4H^-). In the $Cr_2O_y^-$ envelope, the significant ions were *m/z* 168 ($Cr_2O_4^-$), *m/z* 169 ($Cr_2O_4H^-$), *m/z* 184 ($Cr_2O_5^-$), *m/z* 185 ($Cr_2O_5H^-$), 186 ($Cr_2O_5H_2^-$), *m/z* 200 $(Cr_2O_6)^-$, *m/z* 201 ($Cr_2O_6H^-$) and *m/z* 202 ($Cr_2O_6H_2^-$). Envelopes of ions having the general compositions $Cr_3O_6H_z^-$ and $Cr_3O_7H_z^-$ were observed at masses beginning at *m/z* 252 and 268, respectively. Prominent Cr_1 and Cr_2 oxyanions were subjected to ion isolation, and allowed to react with O_2 at pressures between 0.5–2 $\times$ 10^{-6} torr. The abundances of the H-bearing ions in the $Cr_2O_yH_z^-$ envelopes, and of the $Cr_3O_yH_z^-$ species decreased quickly with primary ion dose independent of any ion-molecule reactions. For this reason, they were difficult to isolate, and a rigorous investigation of reaction pathways and measurement of kinetics for these species was not attempted.

$Cr_1O_yH_z^- + O_2$

Four ions were evaluated for reaction with O_2, viz., CrO_2^-, CrO_3^-, CrO_4^-, and CrO_4H^-. Of these, only CrO_2^- underwent measurable reaction over the course of 2.0 s, which was the maximum time the data system allows per scan function. Isolation of CrO_2^- (*m/z* 84) followed by reaction with 8 $\times$ 10^{-7} torr O_2 resulted primarily in formation of CrO_3^- at *m/z* 100 (Reaction 1, Figure 2). A very low abundance ion was also observed at *m/z* 102, which corresponded to $CrO_3H_2^-$ and arose from an inefficient addition reaction with trace residual H_2O in the ion trap [29]. Reaction 1 was modeled as an apparent bimolecular reaction, having a rate constant (k_1) of 3 $\times$ 10^{-10} cm^3 mol^{-1} s^{-1}, which equated to a 38% efficiency compared with the Langevin collision constant (Figure 3).

$$CrO_2^- + O_2 \xrightarrow{k_1} CrO_3^- + O \quad (1)$$

The other three ions that comprise the $Cr_1O_yH_z^-$ enve-

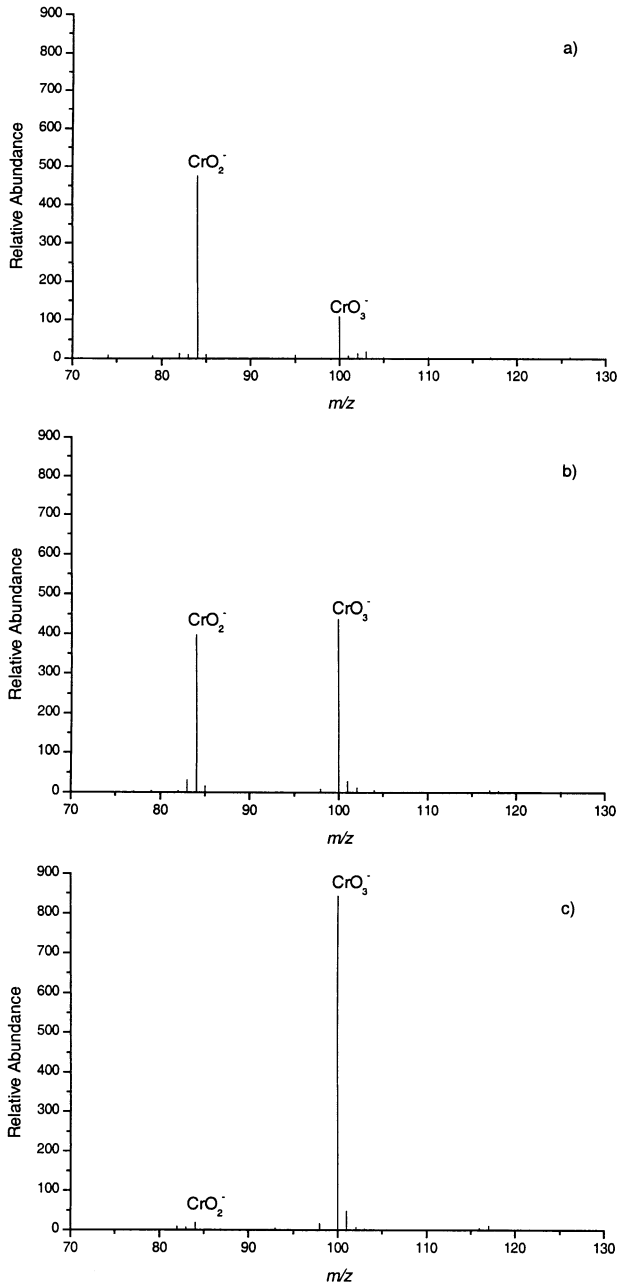

Figure 2. Anion IT-SIMS spectra from addition reaction of isolated CrO_2^- (*m/z* 84) with O_2 pressure of 8×10^{-7} torr (ion gauge). Reaction times of (**a**) 0 s, (**b**) 0.15 s, and (**c**) 1.0 s.

lope in the IT-SIMS spectrum were not observed to undergo any reaction with O_2. We estimated that the slowest reactions observable in the IT-SIMS had rate constants on the order of 1×10^{-12} cm^3 molecule^{-1} sec^{-1}, and therefore if reactions are occurring they must have rate constants less than this value. The failure of the trigonally coordinated CrO_3^- to react contrasted with the behavior of trigonally coordinated metal centers found in $Cr_2O_yH_z^-$ systems, which displayed considerable reactivity with O_2. CrO_3^- evidently enjoys considerable stability compared with other gas-phase Cr oxyanions; this stability is in accord with the finding

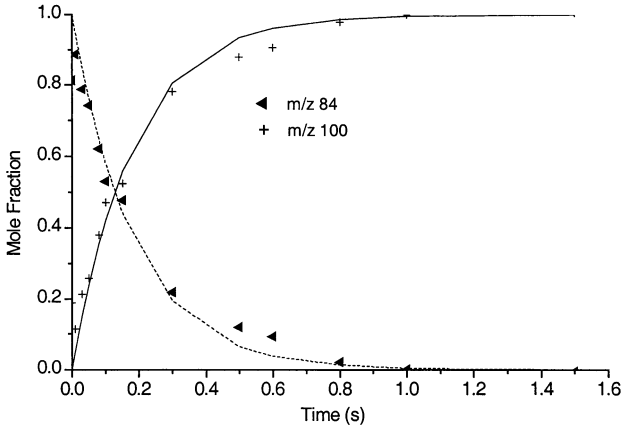

Figure 3. Kinetic profile and selected ion channel data for parent ion CrO_2^- (*m/z* 84) reaction with excess O_2.

that CrO_3^- is normally the most abundant ion in desorption ionization spectra of Cr oxide-bearing surfaces [4, 5, 15, 17, 18].

$Cr_2O_yH_z^- + O_2$

Ions in the $Cr_2O_yH_z^-$ envelope that contained undercoordinated Cr centers (coordination <4) were reactive with O_2. $Cr_2O_4^-$ reacted with O_2 to form CrO_3^- (*m/z* 100; Figures 4, 5; Reaction 2) which occurred via formation of an unstable or activated $(Cr_2O_6^-)^*$ that underwent rapid dissociation to form CrO_3^- and CrO_3. This conclusion was supported by CID MS/MS experiments, which showed that CrO_3^- was the sole fragment ion of $Cr_2O_6^-$ [17], and appears to be an anionic analog to the oxidative degradation reactions recently reported for $V_xO_y^+$ species by Schwarz and coworkers [52]. Ab initio calculations of the $Cr_2O_4^-$ indicated that the structure contained a Cr_2O_2 rhombus [29, 31] with pendant O atoms on the Cr centers; if this is correct, then O_2 must disrupt the Cr_2O_2 rhombus in the process of addition, leading to an unstable, acyclic $Cr_2O_6^-$ intermediate. An analysis of the kinetics of the $Cr_2O_4^-$ oxidation reaction using the ALS approach showed that it was about 15% efficient compared with the Langevin constant (Table 1).

$$Cr_2O_4^- + O_2 \xrightarrow{k_2} CrO_3^- + CrO_3 \quad (2)$$

Also occurring in this experiment was an addition of residual H_2O to $Cr_2O_4^-$, forming $Cr_2O_5H_2^-$ (*m/z* 186; Figure 4b; Reaction 3) in parallel with the oxidation. The kinetic analysis showed the H_2O addition to be 9% efficient (compared to the reparameterized average dipole orientation [49] collision constant), which was in good agreement with the 7% efficiency determined in a study of the reactivity of $Cr_xOyH_z^-$ with H_2O [29]. At longer reaction times (< 2s) (Figure 4c), *m/z* 200 and 204 were observed, which corresponded to $Cr_2O_6^-$ and $Cr_2O_6H_4^-$. An examination of the kinetic profiles *m/z* 200 and 204 (Figure 5) showed that they were products of

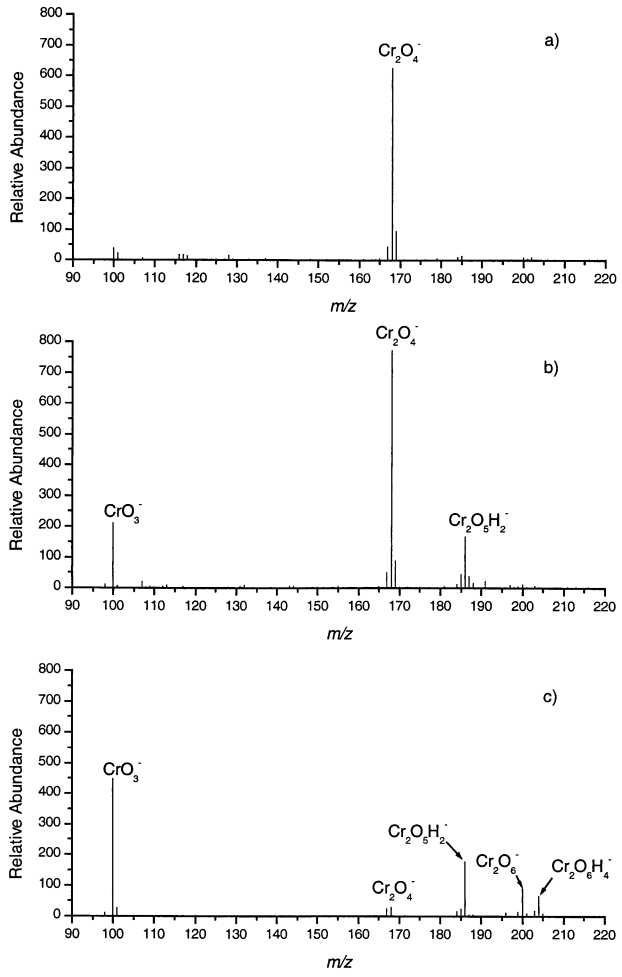

Figure 4. Anion IT-SIMS spectra from addition reaction of isolated $Cr_2O_4^-$ (*m/z* 168) with O_2 pressure of 1.6×10^{-6} torr (ion gauge). Reaction times of (**a**) 0 s, (**b**) 0.075 s, and (**c**) 0.35 s.

reactions of $Cr_2O_5H_2^-$ with O_2 and H_2O, respectively, and are represented by Reactions 4 and 5. The oxidation Reaction 4 must proceed by the initial production an activated intermediate $(Cr_2O_7H_2^-)^*$ which rapidly eliminates H_2O to form a stable $Cr_2O_6^-$. The elimination of H_2O may serve to dissipate energy that would otherwise result in oxidative degradation [52] of the $Cr_2O_6^-$ molecule, as was the case for $Cr_2O_6^-$ formed from $Cr_2O_4^-$. Extraction of the rate constant k_4 showed that this oxidation was only ~1/3 as efficient as the initial oxidation reaction of $Cr_2O_4^-$, which indicated that as the coordination around the Cr atoms increased, reaction rates slowed down [23, 33, 42, 53–56]. $Cr_2O_5H_2^-$ also underwent a slow second hydration reaction to form $Cr_2O_6H_4^-$ (Reaction 5), as noted in reference 29.

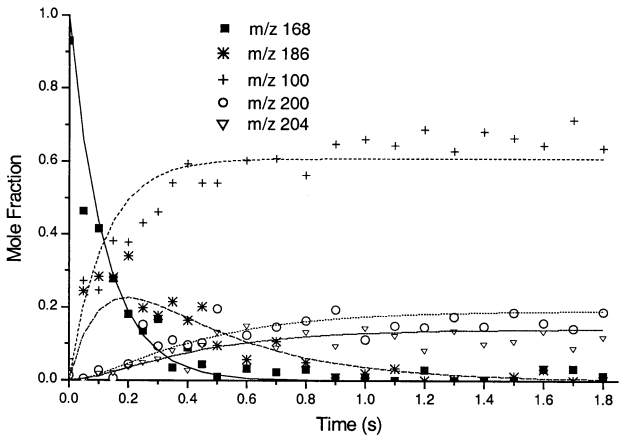

Figure 5. Kinetic profile and selected ion channel data for parent ion $Cr_2O_4^-$ (*m/z* 168) reaction with excess O_2.

$$Cr_2O_4^- + H_2O \xrightarrow{k_3} Cr_2O_5H_2^- \quad (3)$$

$$Cr_2O_5H_2^- + O_2 \xrightarrow{k_4} Cr_2O_6^- + H_2O \quad (4)$$

$$Cr_2O_5H_2^- + H_2O \xrightarrow{k_5} Cr_2O_6H_4^- \quad (5)$$

$Cr_2O_5^-$ (*m/z* 184) also underwent parallel oxidation and hydration reactions, to produce relatively abundant product ions at *m/z* 216, 203, 202, 201, 200, and 185 (Figure 6). Product ions at *m/z* 202 and 201 arose from parallel reactions of $Cr_2O_5^-$ with H_2O, that proceeded via H_2O addition and OH abstraction, respectively [29]. The origin of the ion at *m/z* 202 has some ambiguity because it could arise from OH abstraction by the adjacent ion at *m/z* 185, which was in the IT-SIMS as a result of imperfect ion isolation and from the tendency of $Cr_2O_5^-$ to abstract H. The resultant $Cr_2O_5H^-$ also added H_2O, which accounted for the observation of *m/z* 203, $Cr_2O_6H_3^-$.

The variants of the water reaction did not affect interpretation of the reactions occurring with O_2. Abundant product ions at *m/z* 200 $Cr_2O_6^-$ and *m/z* 216 $Cr_2O_7^-$ clearly correlated with high concentrations of O_2, and were thus formed as oxidation products from $Cr_2O_5^-$ (Reactions 6, 7). The kinetic profile (Figure 7) and ALS analysis of the temporal behavior of the two products $Cr_2O_6^-$ and $Cr_2O_7^-$ indicated that the reactions were occurring in parallel with rate constants that were 2 and 4% efficient compared with Langevin [48].

$$Cr_2O_5^- + O_2 \xrightarrow{k_6} Cr_2O_6^- + O \quad (6)$$

$$Cr_2O_5^- + O_2 \xrightarrow{k_7} Cr_2O_7^- \quad (7)$$

The reactivity behavior of $Cr_2O_5^-$ with O_2 was surprising because of the formation of two oxidation products. This suggested that the reaction was occurring over a range of energetic regimes, perhaps modified by collisional stabilization in the IT-SIMS. A reaction pathway in which an activated $(Cr_2O_7^-)^*$ is initially formed could result in elimination of an O atom, or collisional stabi-

Table 1. Rate information from kinetic evaluation of $Cr_xO_yH_z^-$ species reacting with H_2O and O_2 in the IT-SIMS

(Equation no.) reaction	Reactant *m/z*	Product *m/z*	$k_{individual}$[1,2]	$k_{Langevin}$[1,3]	Reaction efficiency[4]
$Cr_1O_yH_z^-$					
(1) $CrO_2^- + O_2 \rightarrow CrO_3^- + O^\bullet$	84	100	3×10^{-10}	6×10^{-10}	38%
$CrO_3^- + H_2O \rightarrow$ N.R.	100	No reaction[5]		6×10^{-10}	
$CrO_4^- + H_2O \rightarrow$ N.R.	116	No reaction[5]		6×10^{-10}	
$CrO_4H^- + H_2O \rightarrow$ N.R.	117	No reaction[5]		6×10^{-10}	
$Cr_2O_yH_z^-$					
(2) $Cr_2O_4^- + O_2 \rightarrow CrO_3^- + CrO_3$	168	100	1×10^{-10}	6×10^{-10}	15%
(3) $Cr_2O_4^- + H_2O \rightarrow Cr_2O_5H_2^-$	168	186	2×10^{-10}	2×10^{-9}	9%
(4) $Cr_2O_5H_2^- + O_2 \rightarrow Cr_2O_6^- + H_2O$	186	200	4×10^{-11}	6×10^{-10}	6%
(5) $Cr_2O_5H_2^- + H_2O \rightarrow Cr_2O_6H_4^-$	186	204	4×10^{-11}	2×10^{-9}	2%
(6) $Cr_2O_5^- + O_2 \rightarrow Cr_2O_6^- + O^\bullet$	184	200	1×10^{-11}	6×10^{-10}	2%
(7) $Cr_2O_5^- + O_2 \rightarrow Cr_2O_7^-$	184	216	3×10^{-11}	6×10^{-10}	4%
$Cr_2O_6^- + O_2 \rightarrow$ N.R.	200	No reaction[5]		6×10^{-10}	
$Cr_2O_6H_2^- + O_2 \rightarrow$ N.R.	202	No reaction[5]		6×10^{-10}	
$Cr_2O_6H_4^- + O_2 \rightarrow$ N.R.	204	No reaction[5]		6×10^{-10}	

[1]Units are cm^3 $molecule^{-1}$ s^{-1}.
[2]Rate constants were calculated from kinetic modeling.
[3]Langevin collision constant *except* for reactions with H_2O (3 and 5), where the reparameterized average dipole orientation (ADO) constant was used.
[4]$k_{individual}$ as a percentage of $k_{Langevin}$ except in one instance where $k_{individual}$ is expressed as a percentage of k_{rpado} for the water neutral.
[5]Reaction rate constants $<1 \times 10^{-12}$ cm^3 $molecule^{-1}$ s^{-1}.

lization forming stable $Cr_2O_7^-$. If this were the case, one might expect that the kinetic profiles would contain some hint of sequential behavior, but this is not the case. The other alternative is the existence of multiple $Cr_2O_5^-$ reactant ion structures. Oxidation of an acyclic $Cr_2O_5^-$ could result in a reduced dichromate structure containing no rings, and would be attractive because both trivalent Cr atoms in the acyclic $Cr_2O_5^-$ would be susceptible to attack by oxygen. On the other hand, oxidation of a $Cr_2O_5^-$ containing the cyclic Cr_2O_2 rhombus could produce only addition of a single O atom, because in this case only one Cr atom in the reactant ion has a coordination number of <4. We expect structures containing the Cr_2O_2 rhombus to be more stable on the basis of Pandey's DFT calculations [31], and our own Hartree-Fock calculations [29].

The observation of $Cr_2O_7^-$ was also surprising from an oxidation state perspective, because the average oxidation state for Cr in this ion is 6.5. This was the only ion encountered having an average oxidation state > 6, other than CrO_4^-, which had a nominal Cr oxidation state of 7. Since oxidation of Cr beyond the 6 state is unlikely, this indicates localization of a radical electron on a pendant O atom, or a peroxy structure. Both $Cr_2O_7^-$ and CrO_4^- were unreactive with either O_2 or H_2O.

The coordination number of the Cr atoms in the oxyanions plays a more important role in dictating reactivity than does the oxidation state. Tetracoordinate Cr centers are unreactive to further oxidation or hydration in the gas phase, irrespective of oxidation state. For example, neither oxidation nor hydration occur for the tetracoordinate CrO_4^- or CrO_4H^-, and both $Cr_2O_6^-$ or $Cr_2O_6H_4^-$ are similarly inert: Assuming the Cr_2-containing ions possess the Cr_2O_2 rhombus, then they both contain only tetracoordinate Cr centers, but have widely differing average oxidation states (5.5 and 3.5, respectively). The low average oxidation state of Cr in $Cr_2O_6H_4^-$ conveys no reactivity toward O_2.

If the $Cr_2O_4^-$ ion indeed contains the Cr_2O_2 rhombus, two tricoordinate Cr centers are dictated, and the molecule will accommodate two additional O atoms (in the form of O_2 or two H_2O) [29], producing a product ion that contains two tetracoordinate centers, but nothing more coordinated. That the $Cr_2O_4^-$ molecule would fragment on oxidation is somewhat surprising, and indicates that the oxidation process is exothermic enough to break up the Cr_2O_2 rhombus to form two stable products (CrO_3^- and CrO_3). However, noting the non-reactivity of CrO_3^- itself, it is clear that low coordination is not entirely sufficient to motivate reactivity: CrO_3^- represents Cr in the +5 state, so perhaps the generalization can be made that low-coordinate, low-oxidation state metal centers are required for oxidation and/or hydration.

The reactivity of $Cr_2O_5^-$ is intermediate, perhaps reflecting the existence of two structures. $Cr_2O_5^-$ will add only one H_2O, consistent with a single structure. However, it combines with O_2 via two distinct pathways, which suggests the existence of two distinct $Cr_2O_5^-$ structures. The $Cr_2O_5^-$ probably has substantial radical character, since abstractions of H and OH are observed. Radical character would reduce the effective oxidation state of the Cr centers, making both susceptible to oxidation.

Conclusions

The O_2 oxidation reactions of chromium oxyanions proceed along a variety of reaction pathways starting from low-coordinate, low-oxidation state Cr centers. Only Cr centers having coordination numbers <4, *and* oxidation states <5 are reactive toward O_2 (and H_2O).

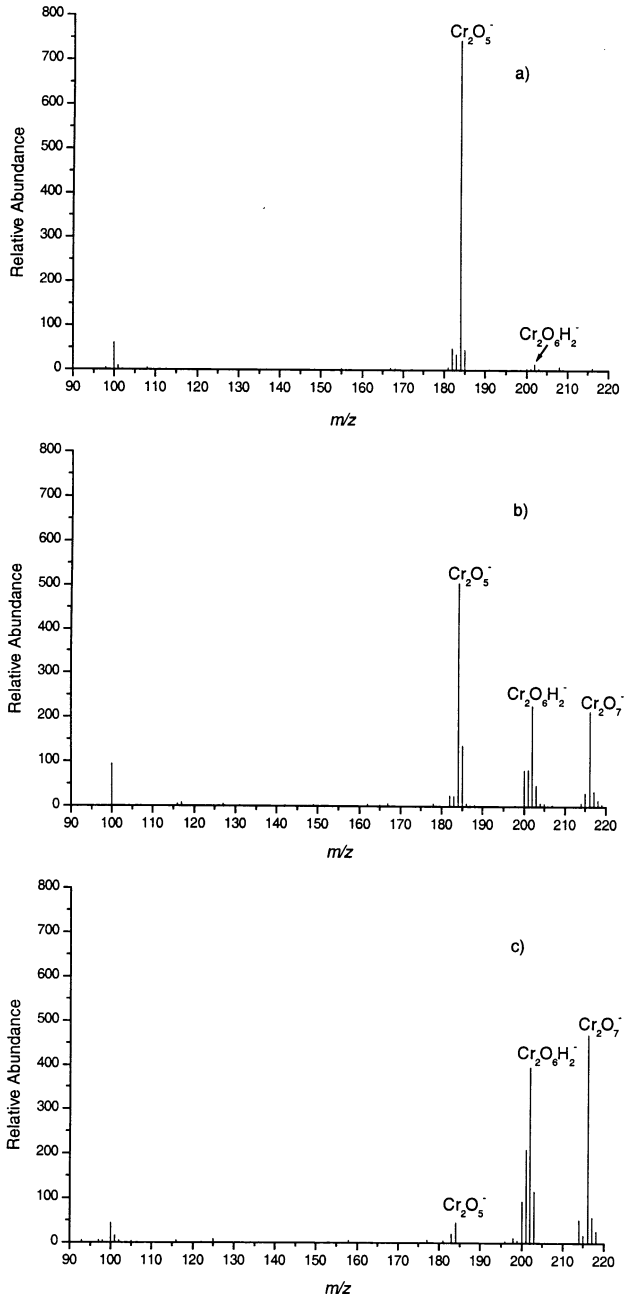

Figure 6. Anion IT-SIMS spectra from addition reaction of isolated $Cr_2O_5^-$ (*m/z* 184) with O_2 pressure of 1.6×10^{-6} torr (ion gauge). Reaction times of (**a**) 0 s, (**b**) 0.20 s, and (**c**) 1.60 s.

Once higher oxidation states and coordination numbers are achieved, further reactivity is halted. Since low valent, low oxidation state metal oxyanions are produced in desorption ionization processes, this suggests that these reactions could play an important role influencing the final distribution of secondary ions observed. Since such low oxidation state and low valent ions tend to be formed from low valent oxide surfaces [19], these would be most easily misidentified as a result of extensive oxidation reactions occurring in the gas phase.

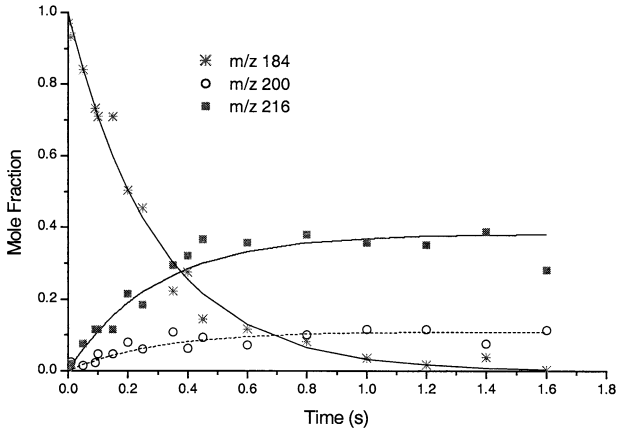

Figure 7. Kinetic profile and selected ion channel data for parent ion $Cr_2O_5^-$ (*m/z* 184) reaction with excess O_2.

Acknowledgment

The authors acknowledge the funding support of the United States Department of Energy, Environmental Systems Research Program, under contract DEAC–07-99ID13727.

References

1. Kimbrough, D. E.; Cohen, Y.; Winer, A. M.; Creelman, L.; Mabuni, C. A Critical Assessment of Chromium in the Environment. *Crit. Rev. Environ. Sci. Technol.* **1999,** *29,* 1–46.
2. Bencko, V. Chromium: A Review of Environmental and Occupational Toxicology. *J. Hyg. Epidimol. Microbiol. Immunol.* **1985,** *29,* 37–46.
3. O'Day, P. A. Molecular Environmental Geochemistry. *Rev. Geophys.* **1999,** *37,* 249–274.
4. Neubauer, K. R.; Johnston, M. V.; Wexler, A. S. Chromium Speciation in Aerosols by Rapid Single-Particle Mass Spectrometry. *Int. J. Mass Spectrom. Ion Processes* **1995,** *151,* 77–87.
5. Poels, K.; Van Vaeck, L.; Gijbels, R. Microprobe Speciation Analysis of Inorganic Solids by Fourier Transform Laser Mass Spectrometry. *Anal. Chem.* **1998,** *70,* 504–512.
6. Aubriet, F.; Maunit, B.; Muller, J.-F. Speciation of Chromium Compounds by Laser Ablation/Ionization Mass Spectrometry and a Study of Matrix Effects. *Int. J. Mass Spectrom.* **2001,** *209,* 5–21.
7. Aubriet, F.; Maunit, B.; Muller, J.-F. Studies on Alkali and Alkaline Earth Chromate by Time-of-Flight Laser Microprobe Mass Spectrometry and Fourier Transform Ion Cyclotron Resonance Mass Spectrometry. Part I: Differentiation of Chromate Compounds. *Int. J. Mass Spectrom. Ion Processes* **2000,** *198,* 189–211.
8. Aubriet, F.; Poleunis, C.; Bertrand, P. Capabilities of Static TOF-SIMS in the Differentiation of First-Row Transition Metal Oxides. *J. Mass Spectrom.* **2001,** *36,* 641–651.
9. Aubriet, F.; Muller, J. F. About the Atypical Behavior of CrO_3, MoO_3, and WO_3 during Their UV Laser Ablation/Ionization. *J. Phys. Chem. A* **2002,** *106,* 6053–6059.
10. Hachimi, A.; Millon, E.; Poitevin, E.; Muller, J. F. Study of the Hydration Effect and Composition of the Salts on Chromium Cluster Formation by Laser Ablation. *Analysis* **1993,** *21,* 11–19.
11. Hachimi, A.; Poitevin, E.; Krier, G.; Muller, J. F.; Pironon, J.; Klein, F. Extensive Study of Oxidation-States of Chromium in Particles by Lamma and Raman Microprobes—Application to Industrial-Hygiene. *Analusis* **1993,** *21,* 77–82.
12. Hachimi, A.; Poitevin, E.; Krier, G.; Muller, J.-F.; Ruiz-Lopez, M. F. Study of the Mechanism of Chromium Cluster Forma-

tion by Laser Microprobe Mass Spectrometry. Correlation with Theoretical Computations. *Int. J. Mass Spectrom. Ion Processes* **1995,** *144,* 23–45.
13. Hachimi, A.; Van Vaeck, L.; Poels, K.; Adams, F. C.; Muller, J.-F. Speciation of Chromium, Lead, and Nickel Compounds by Laser Microprobe Mass Spectrometry and Application to Environmental and Biological Samples. *Spectrochim. Acta, Part B* **1998,** *53,* 347–365.
14. Van Vaeck, L.; Adriaens, A.; Adams, F. Microscopical Speciation Analysis with Laser Microprobe Mass Spectrometry and Static Secondary Ion Mass Spectrometry. *Spectrochim. Acta, Part B* **1998,** *53,* 367–378.
15. Aubriet, F.; Maunit, B.; Courrier, B.; Muller, J.-F. Studies of the Chromium Oxygenated Cluster Ions Produced During the Laser Ablation of Chromium Oxides by Laser Ablation/Ionization Fourier Transform Ion Cyclotron Resonance Mass Spectrometry. *Rapid Commun. Mass Spectrom.* **1997,** *11,* 1596–1601.
16. Aubriet, F.; Maunit, B.; Muller, J.-F. Studies on Alkali and Alkaline Earth Chromate by Time-of-Flight Laser Microprobe Mass Spectrometry and Fourier Transform Ion Cyclotron Resonance Mass Spectrometry. Part II. Understanding Cluster Ion Formation. *Int. J. Mass Spectrom.* **2000,** *198,* 213–234.
17. Van Stipdonk, M. J.; Justes, D. R.; Schweikert, E. A. Determination of the Metastable Dissociation Pathways for Chromium-Oxygen Cluster Ions Sputtered from Potassium Chromate and Dichromate Using the Ion-Neutral Correlation Method. *Int. J. Mass Spectrom.* **2000,** *203,* 59–69.
18. Benninghoven, A. Surface Investigation of Solids by the Statistical Method of Secondary Ion Mass Spectroscopy (SIMS). *Surf. Sci.* **1973,** *35,* 427–457.
19. Plog, C.; Wiedmann, L.; Benninghoven, A. Empirical Formula for the Calculation of Secondary Ion Yields from Oxidized Metal Surfaces and Metal Oxides. *Surf. Sci.* **1977,** *67,* 565–580.
20. Van Stipdonk, M. J.; Justes, D. R.; Force, C. M.; Schweikert, E. A. Speciation of Sodium Nitrate and Sodium Nitrite Using Kiloelectronvolt Energy Atomic and Polyatomic and Megaelectronvolt Energy Atomic Projectiles with Secondary Ion Mass Spectrometry. *Anal. Chem.* **2000,** *72,* 2468–2474.
21. Frenkel, A. I.; Hills, C. W.; Nuzzo, R. G. A View from the Inside: Complexity in the Atomic Scale Ordering of Supported Metal Nanoparticles. *J. Phys. Chem. B* **2001,** *105,* 12689–12703.
22. Zachara, J. M.; McKinley, J. P. Influences of Hydrolysis on the Sorption of Metal Cations by Smectites: Importance of Edge Coordination Reactions. *Aquat. Sci.* **1993,** *44,* 250–261.
23. Dinca, A.; Davis, T. P.; Fisher, K. J.; Smith, D. R.; Willett, G. D. Vanadium Oxide Anion Cluster Reactions with Methyl Isobutyrate and Methyl Methacrylate Monomer and Dimer: A Study by FT/ICR Mass Spectrometry. *Int. J. Mass Spectrom. Ion Processes* **1999,** *183,* 73–84.
24. Appelhans, A. D.; Delmore, J. E. Comparison of Polyatomic and Atomic Primary Beams for Secondary Ion Mass-Spectrometry of Organics. *Anal. Chem.* **1989,** *61,* 1087–1093.
25. Van Stipdonk, M. J.; Justes, D. R.; Santiago, V.; Schweikert, E. A. A Comparison of Ion Emission from $NaNO_3$ Produced by KeV Energy Atomic and Polyatomic Primary Ions. *Rapid Commun. Mass Spectrom.* **1998,** *12,* 1639–1643.
26. Harris, R. D.; Van Stipdonk, M. J.; Schweikert, E. A. Kiloelectron Volt Cluster Impacts: Prospects for Cluster-SIMS. *Int. J. Mass Spectrom.* **1998,** *174,* 167–177.
27. Groenewold, G. S.; Delmore, J. E.; Olson, J. E.; Appelhans, A. D.; Ingram, J. C.; Dahl, D. A. Secondary Ion Mass Spectrometry of Sodium Nitrate: Comparison of ReO_4^- and Cs^+ Primary Ions. *Int. J. Mass Spectrom. Ion Processes* **1997,** *163,* 185–195.
28. Brodbelt, J. S. Effects of Collisional Cooling on Ion Detection. *In Practical Aspects of Ion Trap Mass Spectrometry;* March, R. E.; Todd, J. F. J., Eds.; CRC Press: New York, 1995; pp 209–220.
29. Gianotto, A. K.; Hodges, B. D. M.; Benson, M. T.; Harrington, P. B.; Appelhans, A. D.; Olson, J. E.; Groenewold, G. S. Ion-Molecule Reactions of Gas-Phase Chromium Oxyanions: $Cr_xO_yH_z^- + H_2O$. *J. Phys. Chem. A*, in press.
30. Chertihin, G. V.; Bare, W. D.; Andrews, L. Reactions of Laser-Ablated Chromium Atoms with Dioxygen. Infrared spectra of CrO, OCrO, CrOO, CrO_3, $Cr(OO)_2$, Cr_2O_2, Cr_2O_3, and Cr_2O_4 in Solid Argon. *J. Chem. Phys.* **1997,** *107,* 2798–2806.
31. Xiang, K.-H.; Pandey, R.; Recio, J. M.; Francisco, E.; Newsam, J. M. A Theoretical Study of the Cluster Vibrations in Cr_2O_2, Cr_2O_3 and Cr_2O_4. *J. Phys. Chem. A* **2000,** *104,* 990–994.
32. Bricker, D. L.; Russell, D. H. A Study of the Ion-Molecule Reactions of the $Cr(CO)_5^-$ Anion with Oxygen. *J. Am. Chem. Soc.* **1987,** *109,* 3910–3916.
33. Scott, J. R.; Groenewold, G. S.; Gianotto, A. K.; Benson, M. T.; Wright, J. B. Experimental and Computational Study of Hydration of Reactions of Aluminum Oxide Anion Clusters. *J. Phys. Chem. A* **2000,** *104,* 7079–7090.
34. Groenewold, G. S.; Hodges, B. D. M.; Scott, J. R.; Gianotto, A. K.; Appelhans, A. D.; Kessinger, G. F.; Wright, J. B. Oxygen-for-Sulfur Exchange in the Gas-Phase: Reactions of Al and Si Oxyanions with H_2S. *J. Phys. Chem. A* **2001,** *105,* 4059–4064.
35. Gresham, G. L.; Gianotto, A. K.; Harrington, P. B.; Cao, L.; Scott, J. R.; Olson, J. E.; Appelhans, A. D.; Van Stipdonk, M. J.; Groenewold, G. S. Gas-Phase Hydration of U(IV), U(V), and U(VI) Dioxo Monocations. *J. Phys. Chem. A*, unpublished.
36. Groenewold, G. S.; Appelhans, A. D.; Ingram, J. C. Characterization of Bis(Alkylamine)Mercury Cations From Mercury Nitrate Surfaces by Using an Ion Trap Secondary Ion Mass Spectrometer. *J. Am. Soc. Mass Spectrom.* **1998,** *9,* 35–41.
37. Van Stipdonk, M. J.; Santiago, V.; Schweikert, E. A. Negative Secondary Ion Emission from NaBF4: Comparison of Atomic and Polyatomic Projectiles at Different Impact Energies. *J. Mass Spectrom.* **1999,** *34,* 554–562.
38. Bartmess, J. E.; Georgiadis, R. M. Empirical Methods for Determination of Ionization Gauge Relative Sensitivities For Different Gases. *Vacuum* **1983,** *33,* 149–153.
39. Todd, J. F. J. Introduction to Practical Aspects of Ion Trap Mass Spectrometry. *In Practical Aspects of Ion Trap Mass Spectrometry;* March, R. E.; Todd, J. F. J., Eds.; CRC Press: New York, 1995; p 4.
40. Peschke, M.; Blades, A. T.; Kebarle, P. Hydration Energies and Entropies for Mg^{2+}, Ca^{2+}, Sr^{2+}, and Ba^{2+} from Gas-Phase Ion-Water Molecule Equilibria Determinations. *J. Phys. Chem. A* **1998,** *102,* 9978–9985.
41. Weishaar, J. C. Bare Transition Metal Atoms in the Gas-Phase: Reactions of M, M^+, and M^{2+} with Hydrocarbons. *Acc. Chem. Res.* **1993,** *26,* 213–219.
42. Combariza, M. Y.; Vachet, R. W. Gas-Phase Ion-Molecule Reactions of Transition Metal Complexes: The Effect of Different Coordination Spheres on Complex Reactivity. *J. Am. Soc. Mass Spectrom.* **2002,** *13,* 813–825.
43. Harrington, P. B.; Gianotto, A. K.; Hodges, B. D. M.; Groenewold, G. S. Multivariate Kinetic Modeling of Ion Trap Mass Spectra, unpublished.
44. Windig, W.; Guilment, J. Interactive Self-Modeling Mixture Analysis. *Anal. Chem.* **1991,** *63,* 1425–1432.
45. de Juan, A.; Maeder, M.; Martinez, M.; Tauler, R. Combining Hard- and Soft-Modeling to Solve Kinetic Problems. *Chemometrics Intell. Lab. Syst.* **2000,** *54,* 123–141.
46. de Juan, A.; Maeder, M.; Martinez, M.; Tauler, R. Application of a Novel Resolution Approach Combining Soft- and Hard-Modeling Features to Investigate Temperature-Dependent Kinetic Processes. *Anal. Chim. Acta* **2001,** *442,* 337–350.

47. Nelder, J. A.; Mead, R. A. A Simplex Method for Function Minimization. *Comput. J* **1965,** *7,* 308–313.
48. Gioumousis, T.; Stevenson, D. P. Reactions of Gaseous Molecule Ions with Gaseous Molecules. V. Theory. *J. Chem. Phys.* **1958,** *29,* 294.
49. Su, T.; Chesnavich, W. J. Parametrization of the Ion-Polar Molecule Collision Rate Constant by Trajectory Calculations. *J. Chem. Phys.* **1982,** *76,* 5183–5185.
50. Goeringer, D. E.; McLuckey, S. A. Relaxation of Internally Excited High-Mass Ions Simulated Under Typical Quadrupole Ion Trap Storage Conditions. *Int. J. Mass Spectrom. Ion Processes* **1998,** *177,* 163–174.
51. Gronert, S. Estimation of Effective Ion Temperatures in a Quadrupole Ion Trap. *J. Am. Soc. Mass Spectrom.* **1998,** *9,* 845–848.
52. Engeser, M.; Weiske, T.; Schroder, D.; Schwarz, H. Oxidative Degradation of Small Cationic Vanadium Clusters by Molecular Oxygen: On the Way from V_n^+ (n = 2-5) to VO_m^+ (m = 1-2). *J. Phys. Chem. A* **2003,** *107,* 2855–2859.
53. Gibson, J. K.; Haire, R. G. Synthesis and Investigation of Plutonium Oxide Cluster Ions: $Pu_xO_y^+$ ($x \leqq 18$). *J. Alloy. Compound* **2001,** *322,* 143–152.
54. Groenewold, G. S.; Scott, J. R.; Gianotto, A. K.; Hodges, B. D. M.; Kessinger, G. F.; Benson, M. T.; Wright, J. B. Gas-Phase Condensation Reactions of Si_xO_y H_z^- Oxyanions with H_2O. *J. Phys. Chem. A* **2001,** *105,* 9681–9688.
55. Squires, R. R. Gas-Phase Transition-Metal Negative Ion Chemistry. *Chem. Rev.* **1987,** *87,* 623–646.
56. Zemski, K. A.; Justes, D. R.; Castleman, Jr., A. W. Studies of Metal Oxide Clusters: Elucidating Reactive Sites Responsible for the Activity of Transition Metal Oxide Catalysts. *J. Phys. Chem. B* 2002, **106**, 6136–6148.